Measurement Technique for Sea Height of Burst Using Image Recognition

Ju Ho Choi, Sung Soo Hong, Kyu-Chang Kang, and Joon Lyou

Abstract : A measurement technique of a sea height of burst is introduced for a proximate test using the image recognition of video cameras. In the burst of fuse on the ocean, the burst center of fuse, the sea surface level and the height of calibration poles are measured by the process of image obtained from cameras. Finally, the height of burst of fuse can be computed by Hough transform algorithm. The error compensation algorithms are proposed to eliminate the errors caused by camera level and environmental parameters. As a result of experiment, it has been proved that the proposed measurement system shows the recognition of the center point of the burst image with ±0.5 m error.

Keywords : sea height of burst, image recognition

I. Introduction

When the projectile leaves the muzzle of the gun, the proximity fuse busts at the settled falling level of the projectile away from the sea surface. The reflection factor and the height of burst (HOB) are a little different whether the reflective surface is the ground or the sea. This paper proposes a measurement technique specific to sea surface test.

When the proximity fuse bursts, light, heat, burst sound and flames occur for a very short time and water poles are formed, because the fragments of the projectile spread out on the sea surface simultaneously. The difficult things related to the measurement of the HOB are as follows: 1) the burst position of the fuse depends on the type of projectile, 2) the burst of the fuse appears too far away, 3) there are environmental conditions, such as mist, wave and wind. Since the live shell is used in the fuse test, a danger factor exists, and the measurement is not available from a short distance.

There are two different kinds of the measurement techniques of the HOB in the fuse test: an electro-optical tracking system (EOTS) and a video camera measuring system. The EOTS is a fixed system and is affected by the change in weather condition, but the video camera technique is mobile and compact and has high measurement efficiency Thus, within a measurement environment mentioned above, the image measuring system with a higher zoom lens and a high recording density is required to improve measurement accuracy and to detect the instant of the phenomenon of burst.

In the short distance test, the EOTS has the following defects : 1) the tracking rate of the burst image is kind of low, 2) it takes too much time to process image data, 3) the measurement accuracy tends to be bad owing to the drift of sea level.

To compensate for the above problems, an expanded technique with a zoom lens (300mm×2) is utilized to eliminate ultra-frequency noise on the image that occurs around the edge of the image and a charged coupled device (CCD) camera is equipped with the system to acquire an image with high resolution and a minimum of image distortion

A stable and distinct static image can be obtained using jog-shuttle U-matic VCR. By setting the position of photograph to about 80m above sea level, heat aging of the image induced by mist decreases and the shadow phenomenon from sea surface caused by wave and horizon line is reduced. In addition, the better environment leads to the improved acquisition of the image, and the improved data processing results in the better data processing, image resolution and measurement accuracy.

In this paper, the measurement technique of the HOB on the sea surface uses as follows: a video camera for the image acquisition of burst point, a laser beam range finder which is used to measure the distance between a camera and a burst point, and some calibration poles built on the ocean for distance calibration. This technique offers better features than others: better accuracy, more efficient performance of test and measurement and a mobile type, which is not limited to the measurement area.

Manuscript received : April. 14, 1999., Accepted : Nov. 5, 1999.

Ju Ho Choi, Sung Soo Hong, Kyu Chang Kang : Agency for Defense Development

Joon Lyou : Department of electronics engineering, Chungnam National university

II. Principle of measurement

1. Perspective projection model of pinhole

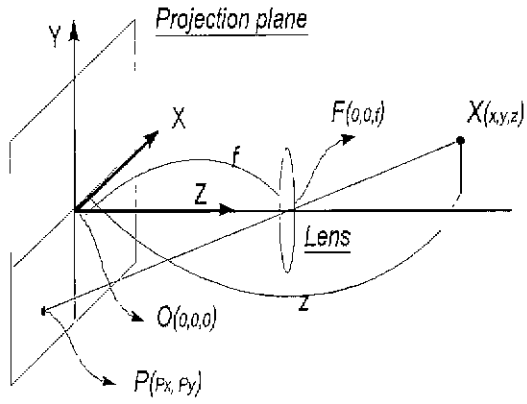

Fig. 1. Perspective projection model of pinhole.

The video camera is composed of a zoom lens and the CCD. The principle of producing the photograph can be explained by the plane perspective projection with pinhole and plane shown in Fig. 1[1, 2].

In Fig. 1, *F(0, 0, f)* is the center of the pinhole of one point *(x, y, z)* in the space, let the perspective projection point coordinate of the perspective projection plane with the center point

$O(0, 0, 0)$ of the pinhole center $F(0, 0, f)$ be $P(P_x, P_y)$. the relation between the points to be projected $X(x, y, z)$ and the perspective projection point $P(P_x, P_y)$ is expressed as

$$P_x = \frac{f \cdot x}{z - f} \approx \frac{f \cdot x}{z} \ (z >> f) \tag{1}$$

$$P_y = \frac{f \cdot y}{z - f} \approx \frac{f \cdot y}{z} \ (z >> f) \tag{2}$$

2. Modeling of the CCD camera

When the perspective projection model of the pinhole corresponds to the zoom lens and the CCD, we find that the pinhole corresponds to the lens with zoom, the perspective projection plane to the plane of the CCD, and the point to be projected to one point on the image plane. In the photograph of a burst, the perspective projection plane of the CCD is denoted by (3). In the photograph of the reference pole, the perspective projection plane of the CCD is given by (4)

$$P_b = \frac{f_b \cdot H}{D_b}$$
$$\therefore H = \frac{P_b \cdot D_b}{f_b} \tag{3}$$

$$P_r = \frac{f_b \cdot L_r}{D_r}$$
$$\therefore f_b = \frac{P_r \cdot D_r}{L_r} \tag{4}$$

where it is assumed that

AS0) H is the HOB above the sea ;

AS1) P_b is the number of pixel ranging vertically from the center of burst to the sea surface, corresponding to the lowest part of water poles;

AS2) D_b is the straight distance from the lens of the camera to the center of burst;

AS3) f_b is the complicated variable that is defined by the state of camera zoom, the focus distance, and the aspect ratio of the static image obtained by the frame grabber;

AS4) L_r is the practical length of the reference pole;

AS5) D_r is the straight distance from the reference pole to the camera lens;

AS6) P_r is the pixel length of the reference pole on the image plane.

3. Height of burst

The HOB, H can be obtained by combining (4), which is the perspective projection equation of burst image, with (3), which is the equation of the reference pole.

$$H = \frac{L_r \cdot P_b \cdot D_b}{D_r \cdot P_r} \tag{5}$$

In (5), the image preprocessing is required to gain a clear and bright image, since there exist image distortion caused by gossamer webs, image aging caused by mist and image noise produced by waves and the reflection of sunlight. In addition, we have to use the VCR and grabber with higher performance to lessen the quantization error due to image distortion of lens and A/D conversion of image signal, and automation of the recognition procedure of the burst points to minimize human errors.

III. Measurement algorithm and error correction

1 Algorithm of image preprocessing[3]

The image preprocessing in the former stage of image recognition is used to obtain a clear and stable image. The emphasis of the image outline is performed using the unsharp masking of corner weighting and interlacing of the video frame grabber. The de-interlacing processing eliminates noises by unsharpening and in addition, the image histogram improves brightness and contrast of the image.

1.1 Unsharp masking of the edge line of the image

The acquisition of the edge is very important in preprocessing to obtain a clear object. because the edge, the image includes geometric information of the image, depth information and distance information. The effect of the unsharp masking process on the edge is made by 1) putting the original image in the high frequency filter, 2) multiplying the output of high frequency filter by a certain number, and 3) adding it to the original image. The principle of unsharp masking is shown in Fig. 2. The pixel value of the original image and the Laplacian gradient image is given as

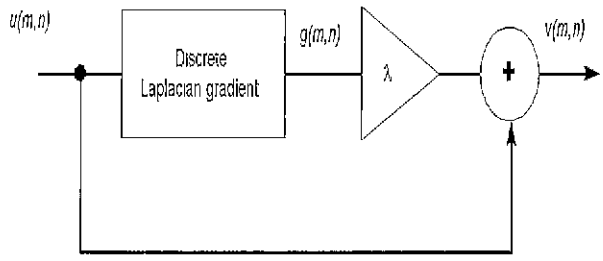

Fig. 2. Principle of unsharp masking

$$v(m,n) = u(m,n) + \lambda \cdot g(m,n) \tag{6}$$

where $v(m,n)$ is the pixel value of result image, $u(m,n)$ is the pixel value of real image, $g(m,n)$ is the pixel value of the Laplacian gradient, and λ is the unsharp masking constant($\lambda>0$) [2, 4]

1 2 De-interlacing

The image interlace generated in the acquisition step of the video static image in the frame grabber must be eliminated since it is produced as noise in the image recognition. The de-interlacing can be computed using the adjacent pixels operation within the image space by 1×4 convolution, and expressed as

$$I_{di}(m,n) = I(m,n) \otimes H(m,n) \tag{7}$$

where $I_{di}(m,n)$ is the gray level of the static image after de-interlacing, $I(m,n)$ is the gray level of the static image before de-interlacing, and $H(m,n)$ is the gray level of the image of the HOB.

1 3 Elimination of binary noise.

The irregular image appears speckled in the burst image. A typical non-linear image filter or a Median filter is applied to eliminate the speckling noises. There are a cross, a square etc. in the shape of the adjacent pixel surface. Among them, since we apply the 3×3 square of adjacent pixels, the filter can be

carried out by redefining the statistical median of nine adjacent images to the respective pixels as a typical pixel.

Let the input pixels of the image $I(x, \theta)$, which is defined as $M \times M$, be $x(m,n)$ and the median of the nine adjacent pixels of $x(m,n)$ be $y(m,n)$. The relative equations between them are expressed as[4][5].

$$y(m,n) = MED\{x(m-1,n-1), x(m-1,n), x(m+1,n), x(m+1,n+1)\} \quad (8)$$

$$x(m,n): 1 \le m, n \le M \quad (9)$$

1 4 Improvement of image contrast

The histogram shows that the relative frequency distribution of the brightness distribution in the 2-D image is displayed in the 1-D graph. The variance value of the histogram is used as a reference to the brightness of image. Thus, (10) and the maximum level of image pixels, v_o can be obtained by improving the image contrast with the redistribution of the original image brightness.

$$v_o = CINT[\frac{v_i - v_{min}}{1 - v_{min}}(L-1) + 0.5] \quad (10)$$

where L is the total level number of image brightness(L=256), v_i is the brightness level of the pixel, v_{min} is the minimum brightness level of pixel within the image, and CINT is the operator of integer conversion.

2. Image recognition algorithm

2.1 Reference object recognition [6]

A reference pole is used for the recognition of the burst image. To obtain the pixel number of reference pole, P_i, from (11), we obtain four edge points of the reference pole P_i (i=1,2,3,4): left upper point P_1, right upper point P_2, left lower point P_3, and P_4 using a mouse. The reference pole is 10.7m high and is about 3,490m away from the measurement point.

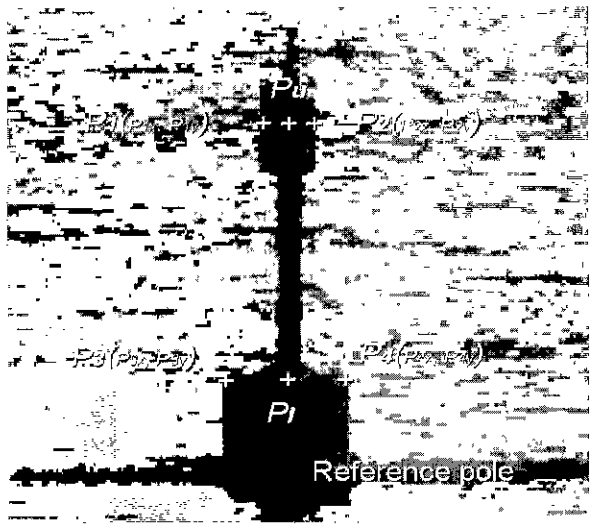

Fig. 3. Reference Pole.

$$\overline{P_i} = \left| \frac{\overline{P_1} + \overline{P_2}}{2} - \frac{\overline{P_3} + \overline{P_3}}{2} \right| \quad (11)$$

where $\overline{P_i}(P_x, \overline{P_y})$ is the amplitude of the corner of reference pole, $\overline{P_u}(P_{ux}, \overline{P_m})$ is the upper amplitude of reference pole, and $\overline{P_l}(P_a, \overline{P_h})$ is the lower amplitude of the reference pole.

2.2 Burst center recognition

A burst flame from the fuse of burst is formed around the center of the burst with circular symmetry. The operation of the burst center is as follows: to catch the initial static image of the burst flame, and then gain segmented image by separating the image flame from the image background, and finally detect the image center of gravity in the burst area.

The recognition procedure of the burst center is shown in Fig. 4. The burst area of interest (BAOI) indicated in Fig 4(a) can be obtained by choosing the flame area of the burst image with a mouse so that the processing time of the image data decreases and the measurement efficiency increases. Finally, the flame image with improved contrast is gained from the preprocessing of partial smoothing of the histogram. The histogram mode method is utilized using the separation phenomenon of the brightness dispersion of the image to divide the image [6, 7].

(a) flame image

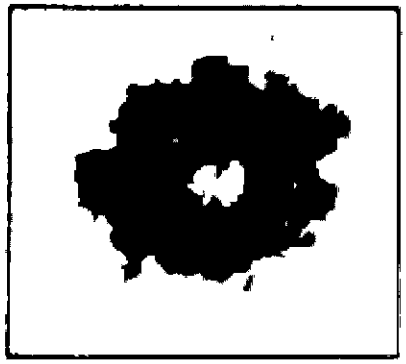

(b) binary image

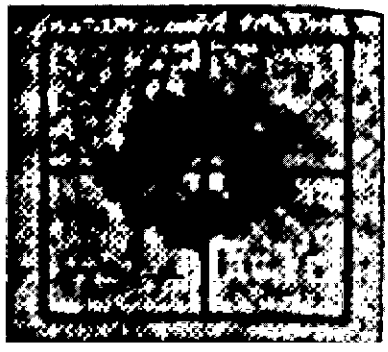

(c) burst recognition

Fig. 4. Image of burst.

The separated brightness dispersion is obtained by deploying the brightness histogram within the BAOI image. If the brightness, which corresponds to the valley of this dispersion, is taken as the threshold value, we can get a binary image like (b). When the ratio of inter-variance between two peaks of the histogram and total variance is maximum, the threshold of the binary image can be acquired from a deterministic analysis method, which determines an arbitrary threshold using only information from the histogram. In the division of the object from the background, and the binary of the supposed threshold k, the classifying degree (CLD), $\eta(k)$ is defined by (12) as the value which evaluates the compatibility of the threshold

$$\eta(k) = \frac{\sigma^2_B(k)}{\sigma^2_T} \tag{12}$$

In the above equation, if the threshold is k, then $\sigma^2_B(k)$ is given as (13) and total variance, σ^2_T as (14)

$$\sigma^2_B(k_{TH}) = \frac{(\mu_t \cdot w(k) - \mu(k))^2}{w(k)\cdot(1-w(k))} \tag{13}$$

$$\sigma^2_T = \sum_{i=1}^{L}(i-\mu_t)^2 P_i \tag{14}$$

Where the total pixel number of the histogram is N, the total level number is L, the probability generated i-level is P_i, and the sum of the expected values up to k level is $\mu(k)$, the following equations are given as

$$p_i = \frac{n_i}{N}, \quad \mu_t = \sum_{i=1}^{L} i \ p_i \tag{15}$$

$$w(k) = \sum_{i=1}^{k} p_i, \quad \mu(k) = \sum i \cdot p_i \tag{16}$$

Since σ^2_T of the classifying degree in (12) is a certain value, then the level, k indicated by the maximum of $\sigma^2_B(k)$ must be regarded as the threshold to obtain optimal threshold, k_{best}

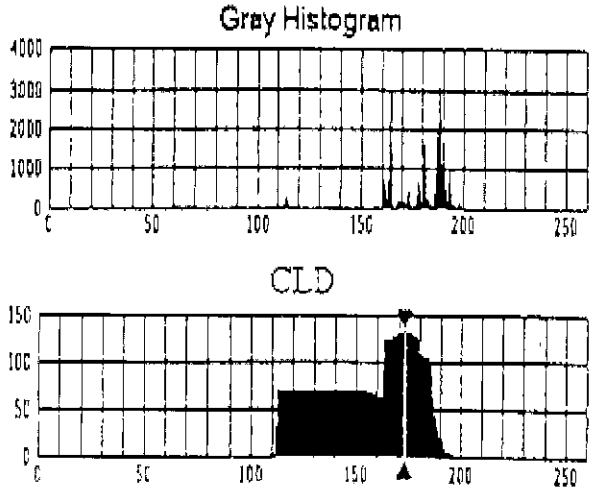

Fig. 5. Gray histogram and CLD of burst image.

When recognizing the burst image with irregular noise, the recognition rate is inaccurate due to spike noise. Thus, the Median filtering is performed to eliminate binary noise included in the binary burst image. Fig. 5 demonstrates the histogram of the flame image and CLD shown in Fig. 4. Then, the CLD is maximum at k=172. The result which is binary-coded by the threshold and carried out by the Median filtering is shown in Fig. 4(b), and the result of the operation of the gravity center of the image is shown in Fig. 4(c).

Let the binary area resulting from the image division be R and the total pixel number within this area be #R, the coordinate of the center of gravity in the second dimension of the image, $B(B_x, B_y)$ is denoted as

$$B_x = \frac{1}{\#R}\sum_{(x,y)\in R} x \tag{17}$$

$$B_y = \frac{1}{\#R}\sum_{(x,y)\in R} y \tag{18}$$

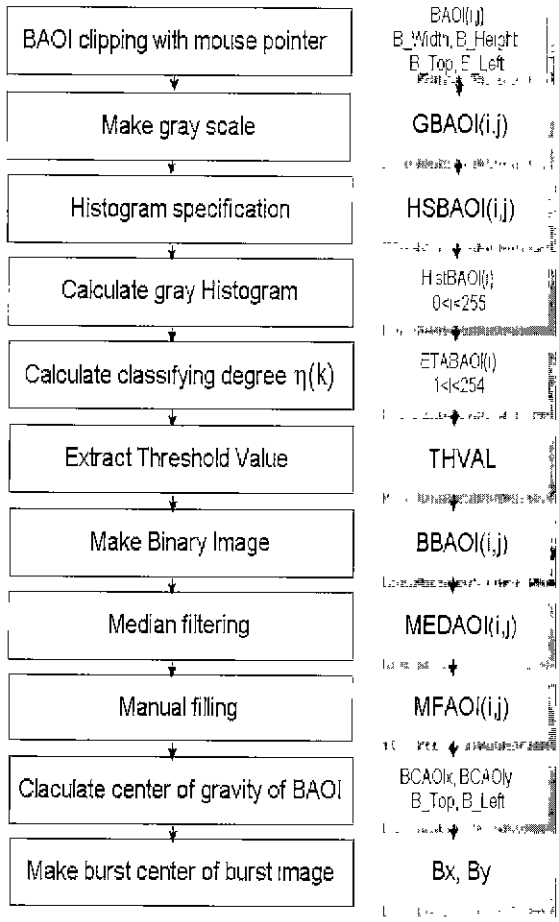

Fig. 6. Recognition procedure of the center of burst point.

Fig. 6 shows the recognition procedure of the center of burst point and input and output parameters.

Recognition of sea surface

The HOB of the fuse, which is the height of the burst point from the sea surface, as well as the recognition of the burst point, gives a strong influence on measurement accuracy. The water pole, which is more than 10m in height and 15m in radius, is formed due to the dispersion of fragments occurring during fuse burst on sea surface. The straight line of the lower part of the water pole consisting of the outline is recognized as the sea surface. The shortest distance between the burst point

and the curved line can be regarded as the HOB, in such case that the sea surface forms a curved line due to wave and wind. Fig. 7 indicates how to detect the sea surface in the primary image.

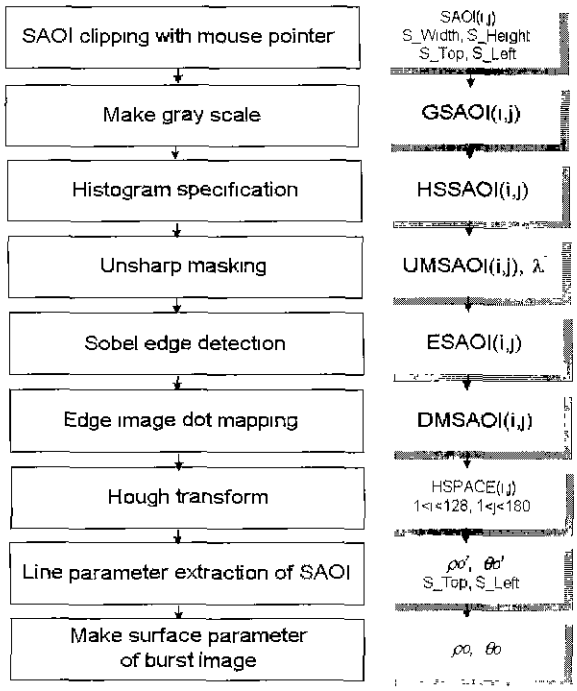

Fig. 7. Detection procedure of sea surface.

Here, the adjacent pixel operation which is used to detect the brightness change of the outline is taken into consideration to detect sea surface and the Sobel operation is used to extract the outline image. The extraction principle of the outline using the Sobel operation is shown in Fig. 8 [8][9].

With 2-D convolution between a downward detection mask, $h_1(m, n)$, an upward detection mask, $h_2(m, n)$ and the image of the sea surface, a central image can be obtained by summing $g_1(m, n)$ and $g_2(m, n)$, and by solving $g(m, n)$. This image is binary-coded by the threshold t, which is about half of the maximum brightness of the medium image, and then the outline image can be obtained by point mapping. The above procedure is the followingr :

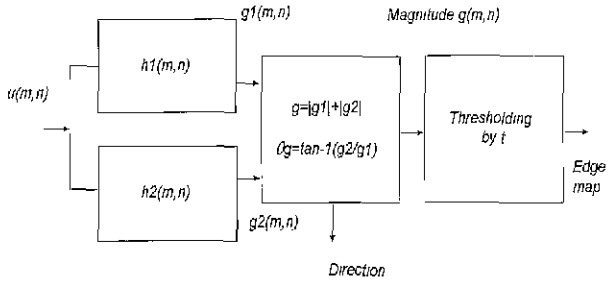

Fig. 8. Edge detection made by Sobel operation.

$$g_1(m,n) = u(m,n) \otimes h_1(m,n) \tag{19}$$

$$g_2(m,n) = u(m,n) \otimes h_2(m,n) \tag{20}$$

$$g(m,n) = \sqrt{g_1^2(m,n) + g_2^2(m,n)} \tag{21}$$

$$g(m,n) = |g_1| + |g_2| \tag{22}$$

where

$$h_1 = \begin{bmatrix} -1 & -2 & -1 \\ 0 & 0 & 0 \\ 1 & 2 & 1 \end{bmatrix}, \quad h_2 = \begin{bmatrix} 1 & 2 & 1 \\ 0 & 0 & 0 \\ -1 & -2 & -1 \end{bmatrix}$$

The Hough transformation is a method of extraction of the image feature that detects geometric information of the image represented in the equation of line, circle and ellipse. In this case, the method becomes a reciprocal linear transformation which maps the feature parameters of the line segment, (ρ_o, θ_o) to one point on the Hough space $H(\rho, \theta)$, where ρ is the vertical distance from the original point to the straight line, θ is the angle between the x-axis and the normal line in the image space.

$$\begin{aligned} &x \cdot \cos\theta + y \cdot \sin\theta = \rho \\ &0 \le \rho \le R, \quad 0 \le \theta \le \pi \end{aligned} \tag{23}$$

The Hough transformation is embodied by the Duda-Hart algorithm. After the Hough transformation of the vertical outline image is extracted from the flame image, the two parameters (ρ, θ) in the Hough space are obtained from normalization between 0 and 1. The angle, θ formed between the normal line and the horizontal line must be limited to 90° ± 5°, because θ of the sea surface is normally 90°. The straight line component which corresponds to the maximum peak within this range, is recognized as the sea surface.

The flowchart of the Hough transformation shown in Fig. 9 is described in detail as follows: 1) first, all parameters in the Hough space, $H(m, n)$ are initialized by the variable declaration of the array of two dimensions, 2) the pixels located on the straight line are accumulated in the Hough space with the accumulation algorithm, 3) the accumulated Hough space is normalized by dividing the maximum element of the array into it so that the accumulated Hough space can be 1 as a maximum value, 4) The maximum peak that indicates the feature

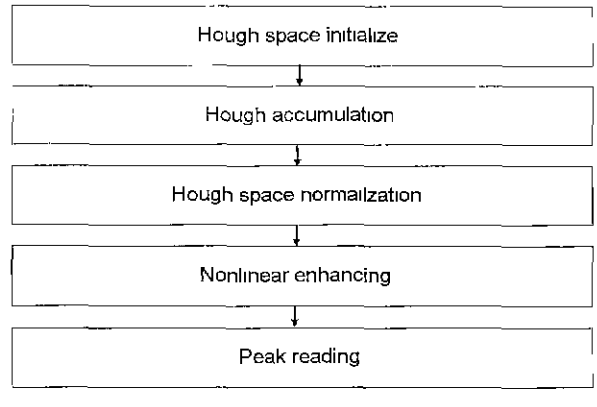

Fig. 9. Procedure of Hough transformation.

parameters of the straight line can be detected, with the non-linear unsharping masking of two dimensional array accumulated from the square operation.

3. Operation of HOB and error compensation

3.1 Operation of HOB

The pixel number of the HOB P_b can be acquired from the burst center, (B_x, B_y) and the variable of the sea surface, (ρ_o, θ_o). One point of the plane, $P(\alpha, \beta)$ and the shortest distance of the straight line, $ax + by = c$, on the same plane, are given by (24) and (25) [1]. In the image tilted a little from the view angle of the camera shown in Fig. 10, the pixel number of the HOB can be computed regardless of angle.

$$D = |\alpha \cdot a + \beta \cdot b - c| \tag{24}$$

$$P_b = |B_x \cdot \cos\theta + B_y \cdot \sin\theta - \rho| \tag{25}$$

With the pixel number of the HOB, P_b, from (26); the distance from a measuring point to a burst point using a range finder, D_b; the pixel number of the reference pole, P_r; the length of the reference pole, L_r; and the distance between the measuring point and the reference pole, D_r, the HOB can be calculated by (5)

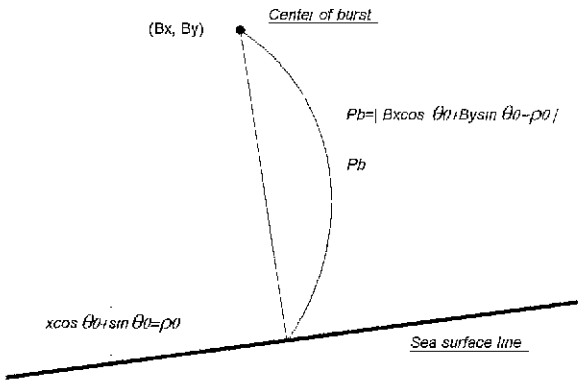

Fig. 10. Minimum HOB.

3.2 Error compensation

There are static errors, dynamic error and load error in the measurement system. Among them, static error forms most of total system error relative to dynamic error and load error. In addition, static error is divided into reading error, environmental error, and characteristic error. The image recognition algorithm can partially eliminate the reading error and characteristic error. Environmental error caused by the change in camera height and the water pole radius can be compensated for by (26). If the HOB indicates H in Fig. 11, H is expressed as

$$H = \frac{H_1}{\cos\alpha} \tag{26}$$

$$\alpha = \sin^{-1}\frac{h}{D_b}$$

$$H_1 = H_2 - \Delta H_1 \tag{27}$$

$$\Delta H_1 = R_b \cdot \sin\alpha \tag{28}$$

where h is the height of a camera from sea level, D_b is the distance between a sea bottom of burst point and a camera, and R_b is a radius of water pole.

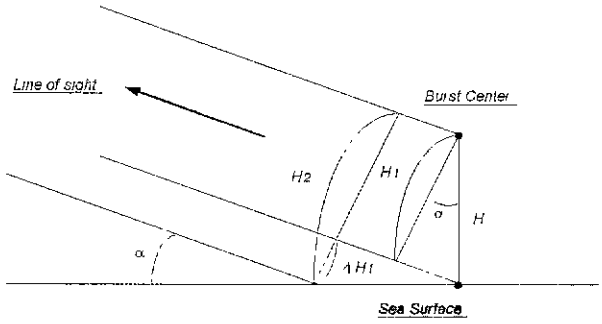

Fig. 11. Principle of error compensation.

Now that the angle, α between the horizontal plane is formed differently by the altitude of the camera and the line of sight of camera is not small so that it can be omitted, the HOB, H ought to be compensated for. H in the above equation is the error-corrected-sea-HOB, and H_2 includes some errors caused by the HOB, H and the radius of water pole, R_b. In (27), the error component produced by only the camera height is found H_1, as ΔH_1 is subtracted from H_2. The relationship between H_1 and H is given by (26) [10].

IV. Test method and measurement result

1 Construction of measurement system

The construction of the measurement system shown in Fig.12 is composed of an image recorder, an image acquisition equipment and an image processing equipment. The image is converted into electrical signals through a color CCTV with 30mm lens, and then is displayed on an image monitor and recorded in a U-matic VCR simultaneously. The recorded image is reproduced by a jog-shuttle U-matic VCR and fed back to a frame grabber for digital image acquisition and finally, sent back to the image processing equipment to further process the image.

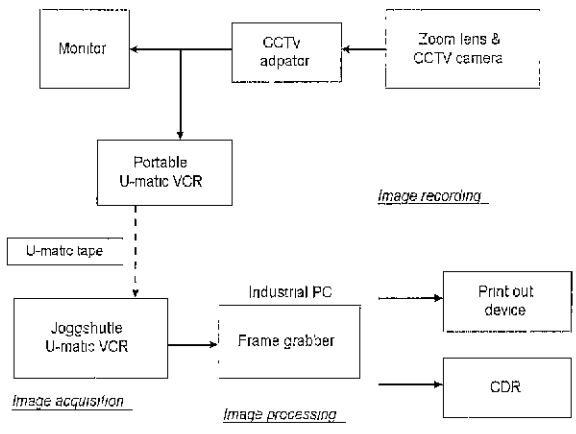

Fig. 12. Block diagram of measurement system.

2. Measurement result

The comparison to the developed video image measurement system and the EOTS has been performed to get measurement result. The burst image of the proximity fuse shown in Fig. 13 includes the sea surface line, the center of burst and the burst flame.

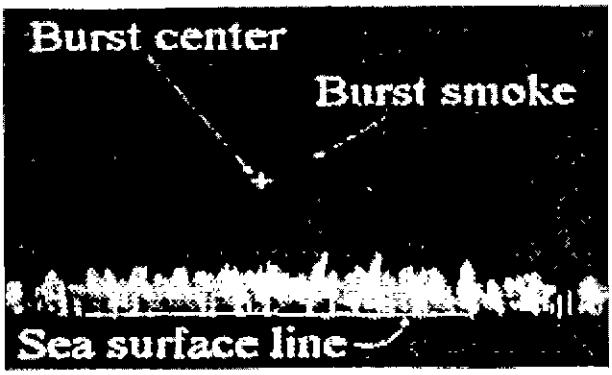

Fig. 13. Burst image of proximity fuze.

Fig. 14 shows the result of the Sobel operation. The recognition result of the straight line corresponding to the maximum peak of the Hough space is represented in Fig. 15. Finally, the result of the Hough transformation is shown in Fig. 16

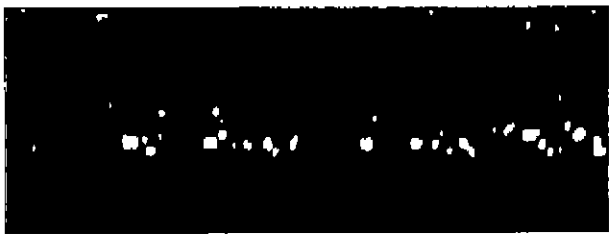

Fig. 14. Result of Sobel operation.

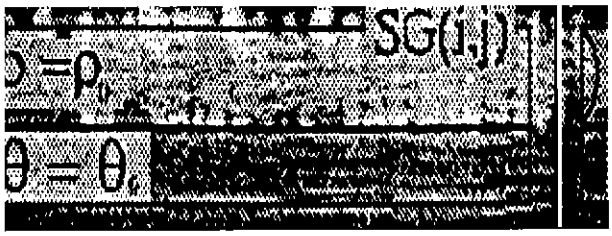

Fig. 15. Result of sea surface operation.

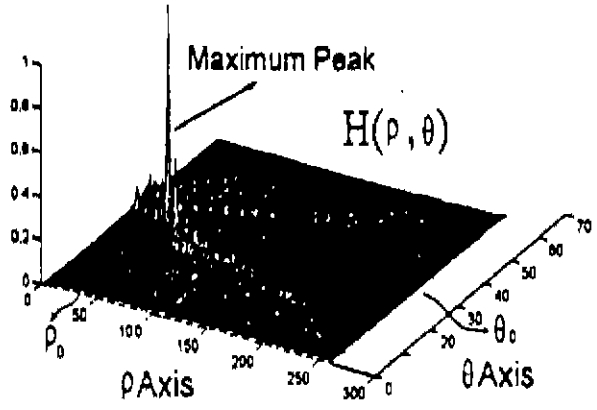

Fig. 16. Hough space of surface edge image.

The burst image of the proximity fuse is divided into type A, type B, and type C according to the caliber of gun and the propellant. A square gate is placed over the flame area and the sea surface area of each image to separate the image area, and then an estimation of the ability of image recognition is carried out using the algorithm outlined in Fig 6 and 7 [11].

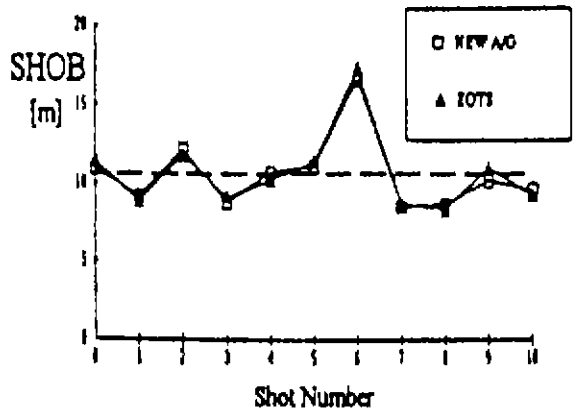

Fig. 17. Type A sea-HOB result compensation.

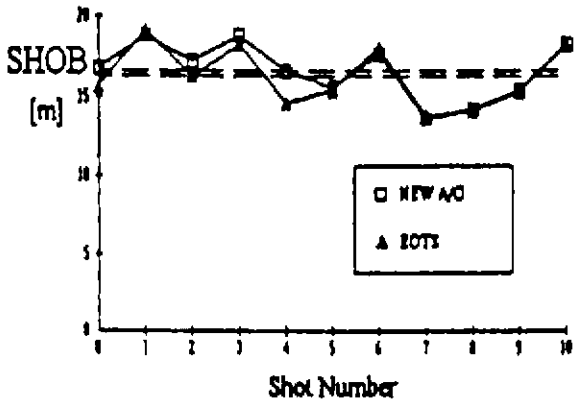

Fig. 18. Type B sea-HOB result comparison.

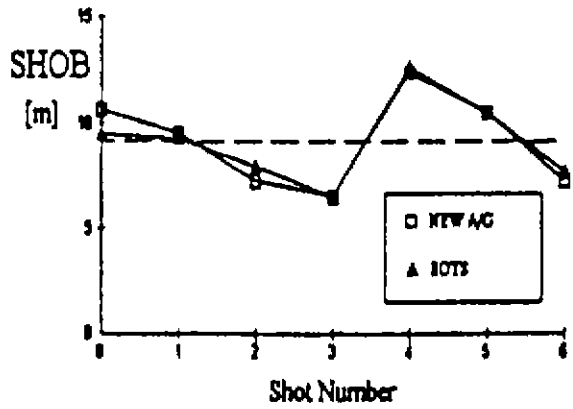

Fig. 19. Type C sea-HOB result comparison.

Fig.17, Fig. 18 and Fig. 19 show a comparison result between the sea-HOB and the EOTS performed with regard to three types: A, B and C. The EOTS is used as a reference to

compare the result. As a result of analysis, the proposed measurement method is superior to the EOTS in measurement accuracy.

V. Conclusion

This paper presents the measurement system of the sea- HOB for the proximity fuse, which is explained by the following algorithm: 1) separates the area of the burst flame from the whole area of captured image, 2) computes the brightness center of the flame for the center of the burst, 3) detects the image outline within the square gate of the lower part of the water pole, 4) performs the Hough transformation, 5) finally, recognizes the sea surface as the straight line between the maximum peaks in the Hough space. As a result of the experiment, it has been proved that the proposed measurement system shows the good recognition of the center point of the burst image with ± 0.5 m error.

In addition, the more advanced algorithm of image processing with high immunity of environmental errors caused by atmosphere unstability, haze, wave is necessary to improve the uncertainty of the system as well as more better image acquisition board and camera capable of high zoom and more than 1,000 frames per second in the future.

References

[1] S. Kahan, T. Pavlidis, and H. S. Baird, "Building a font and size independent character recognition system," *IEEE Trans. on Pattern Analysis and Machine Intelligence*, PAMI-9, pp. 274-288, 1987.

[2] T. Pavlidis and Y. T. Liow, "Integrating region growing and edge detetion," *Proc. IEEE Computer Vision and Pattern Recognition Conf.*, Ann Arbor, Michigan, pp. 6-10, 1988.

[3] B. R. Hunt, "Digital image processing," *Proc* , vol. 63, no. 4, pp. 693-708, 1975.

[4] Daniel I. Barnea and Harvey F. Silverman, "A class of algorithms for fast digital image registration," *IEEE Trans. on Computers*, 1972.

[5] A. Rosenfeld and M. Thurston, "Edge and curve detection for visual scene analysis," *IEEE Trans. on Computers*, 1971.

[6] L. Ernest, *Computer image processing and recognition*, Academic Press, 1979.

[7] G. Andrew, *Applications of digital image processing*, SPIE, vol. 397, 1983.

[8] D. Hart, *Computer vision and image processing*, Willy, 1993.

[9] Steven Harrington, *Computer graphics-a programming approach*, 2nd ED., pp. 223-225, 1980.

[10] Berthold Klaus and Paul Horn, *Robot vision*, MIT Press, pp. 19-26, 1989.

[11] Anil. K. Jain, *Fundamentals of digital image processing*, Prentice Hall, 1989.

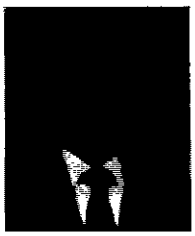

Ju Ho Choi

(1949) received the B. S. degree in electronics engineering from Pusan National University in 1976 and M. S. and Ph. D. degrees in electronics engineering of Chungnam National University in 1993 and 1999 respectively. He is a chief of the development of measurement technique of Agency for Defense Development in Korea. His current research interests include instrumentation system, advanced signal processing and optical fiber communication.

Kyu Chang Kang

He was born in Kyungnam, Korea in 1971. He received the B. S. and M. S degrees in electronics engineering from Kyungpook National University in 1994 and 1997 respectively. He has been involved in the development of the measurement technique for the weapon test in Agency for defense development since 1997. His research interests include image compression, digital signal processing and radar signal processing.

Sung Soo Hong

He was born on November, 1955 in Jeonbuk, Korea. He received the B. S degree in electronics engineering from Sungjeon University in 1981. He has been working on the development of the technique of calibration and measurement for the weapon test in Agency for Defense Development since 1981. He worked for one of U.S Army Proving Ground, Combat Systems Test Activity as an exchange engineer in 1987 and 1988. He has strong interest in the area of dynamic pressure calibration and measurement.

Joon Lyou

(1956) received the B. S. degree in electronics engineering from Seoul National University in 1978, and the M. S. and the Ph. D. degrees from Korea Advanced Institute of Science and Technology in 1980 and 1984 respectively. During the academic year 1989 to 1990 and the year 1997 to 1998, he was a visiting professor at Michigan State University and at University of California at Davis respectively. He has been a professor in the department of electronics engineering of Chungnam National University since 1984. His current research interests include estimation and identification methods for fault detection of control and instrumentation systems, and signal processing.